THE JOURNAL OF PHYSICAL CHEMISTRY C

ARTICLE

pubs.acs.org/JPCC

Evidence for Multiple Trapping Mechanisms in Single CdSe/ZnS Quantum Dots from Fluorescence Intermittency Measurements over a Wide Range of Excitation Intensities

Amy A. Cordones, Teresa J. Bixby, and Stephen R. Leone*

Departments of Chemistry and Physics, University of California and Lawrence Berkeley National Laboratory, Berkeley, California 94720, United States

ABSTRACT: Fluorescence intermittency of single CdSe/ZnS core/shell quantum dot particles is investigated over a wide range of excitation intensities and at two excitation wavelengths. Deviation from previously observed power law behavior in both the on- and off-duration probability distributions is observed at both excitation wavelengths, one near the band gap and one 350 meV above the band gap. Increasing the excitation intensity modifies the off-duration probability distribution such that the probability of long off-time events decreases, an effect that is observed to saturate at an average number of excitons created per pulse of one, $\langle N \rangle \approx 1$. The on-duration probability distribution is well-described by a power law for short on-time events, crossing over to an exponential distribution for long on-time events. Increasing the excitation intensity induces this crossover to occur at earlier times, saturating at $\langle N \rangle \approx 2$. The different intensity-dependent trends for the on- and off-duration probability distributions are evidence that multiple mechanisms govern the blinking statistics, as no single mechanism can account for the different saturation behaviors of the off and on durations as a function of excitation intensity. These mechanisms are assumed to be one based on a light-induced diffusion of both the excited-state and trap state energies (i.e., diffusion-controlled electron transfer) and one that relies on the absorption of multiple photons (i.e., Auger ionization induced trapping).

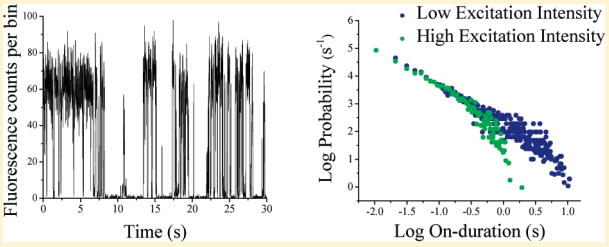

I. INTRODUCTION

The development of semiconductor nanocrystals (NCs) has inspired work across many scientific and application-based fields. Their highly tunable luminescence properties, photostability, small luminescence bandwidth, and high efficiency have already led to the success of NC-based light-emitting devices, such as thin-film light-emitting devices (LEDs).[1−3] These same properties inspire their use in NC-based lasers[4,5] and as fluorescent tags in biological systems.[6] Incorporation of NCs into photovoltaic devices is also promising due to their tunable electronic properties and their relatively inexpensive solution-based device fabrication.[7] The limiting factors in the development of efficient NC-based devices are mainly attributed to a large surface-to-volume ratio that is a result of their very small size. NC−polymer hybrid solar cells, as well as all-inorganic NC solar cells, exhibit efficiencies much lower than is theorized for NC-based photovoltaics, likely due to inefficient charge transfer between the NCs and at the NC−electrode contacts.[8−10] Surface trapping sites such as dangling bonds, lone electron pairs, or crystal defects can localize the electron or hole, thus preventing efficient charge transfer in photovoltaics or band gap recombination in the case of LEDs.

For single NCs the charge-carrier trapping manifests itself as discontinuities in the NC fluorescence under continuous excitation, known as fluorescence intermittency or blinking. The basic blinking mechanism that has become widely accepted involves the localization of a single charge carrier in a trap site that leaves a lone charge in the particle. This lone charge has been thought to induce faster nonradiative recombination processes through energy transfer from any subsequent excitons, thus rendering the particle dark until neutralization of the trapped charge. Recent reports of the off-state quantum yields and nonradiative decay times challenge the charging model altogether.[11,12] The detailed mechanisms of how the charge carrier is trapped, what nonradiative processes occur during the nonfluorescent periods, and how the NC returns to its neutral state are still under investigation. Reviews detailing the various blinking results and proposed mechanisms are available.[13−19] The results reported here focus on the trapping and detrapping processes that lead to the switching between bright and dark states. Specifically, blinking behavior over a larger range of excitation intensities than has been previously reported is analyzed in the framework of several mechanisms.

The initial observations of fluorescence blinking in CdSe NCs by Nirmal et al. prompted proposals for photo- and thermal-ionization based charge trapping mechanisms.[20] Initial models based on Auger ionization required the creation of a multiexciton species through the absorption of more than one photon. The energy released by the annihilation of one exciton could then eject a remaining charge to the surrounding environment, leaving

Received: January 5, 2011
Revised: February 10, 2011
Published: March 07, 2011

the NC in a charged state.[21] Although this mechanism was backed by several early reports of excitation power-dependent blinking, it is inconsistent with the highly distributed blinking behavior observed. The probability distributions of both the on- and off-time durations are well-described by inverse power laws,[22,23] whereas the photoionization models predict a single trapping rate constant and an exponential distribution of on-event durations.[21]

Models that were successful in predicting power law behavior in both the on- and off-duration statistics introduce some diffusing coordinate into the blinking mechanism, caused by fluctuations in the NC environment. A variety of models based on a random walk were proposed, as the wait time to return to the starting point decays by a power law with the same exponent observed in the blinking statistics, −3/2. Early models predicted a random walk of the trap state energy levels, thus creating fluctuations in the tunneling barrier from the excited state to the trap state.[23] Tang and Marcus proposed a similar random walk based model: diffusion-controlled electron transfer (DCET),[24] described in more detail here. This model not only predicts the power law blinking behavior but also the exponential cutoffs that are observed in the probability distributions of long on- and off-durations. In DCET local charge rearrangements induce diffusion of the excited-state energy level. The energy difference between the excited (bright) state and a charged (dark) state is also diffusing. A random walk along assumed parabolic free energy surfaces representing these bright and dark states induces a switch from on to off (or off to on) at each crossing of their intersection. The parabolic shape of the energy surfaces leads to a saturation of the on- and off-duration probabilities and induces a crossover from power law behavior to an exponential decay. The crossover time depends on several experimental parameters such as chemical composition, temperature, and excitation intensity.

Several previous studies have indicated various power-dependent trends in the on- and off-duration probability distributions.[20,23,25−32] A linear power dependence in the on-duration crossover rate is reported by several groups and is predicted by the DCET model.[25,30,31] A quadratic power dependence of the crossover rate was observed and attributed to Auger ionization induced trapping, as that mechanism depends on the creation of a multiexciton species.[28] A lack of a power dependence at low excitation fluxes was reported in earlier work in our laboratory and was attributed to a self-trapping mechanism.[33,34]

The power-dependent studies cited above were performed with very low excitation power densities, well below any saturation that one might expect to see at higher powers. Here the blinking statistics of CdSe/ZnS core/shell quantum dots (QDs) are measured over a larger range of excitation power densities, corresponding to an average of 0.15 excitons to more than 3 excitons created per excitation pulse, $\langle N \rangle$. Saturation of intensity-dependent trends in the crossover times of both on- and off-duration probability distributions is observed here, indicating that the off-duration statistics saturate above $\langle N \rangle = 1$, a single exciton, and the on-duration statistics saturate above $\langle N \rangle = 2$, a biexciton. This asymmetry in the average number of excitons for saturation between off and on durations suggests that multiple mechanisms affect the blinking behavior, as there is no single mechanism that predicts different intensity-dependent behaviors in the detrapping and trapping processes. The mechanisms that are invoked here to describe the on- and off-blinking behavior are a diffusion-based mechanism and an Auger ionization induced trapping mechanism.

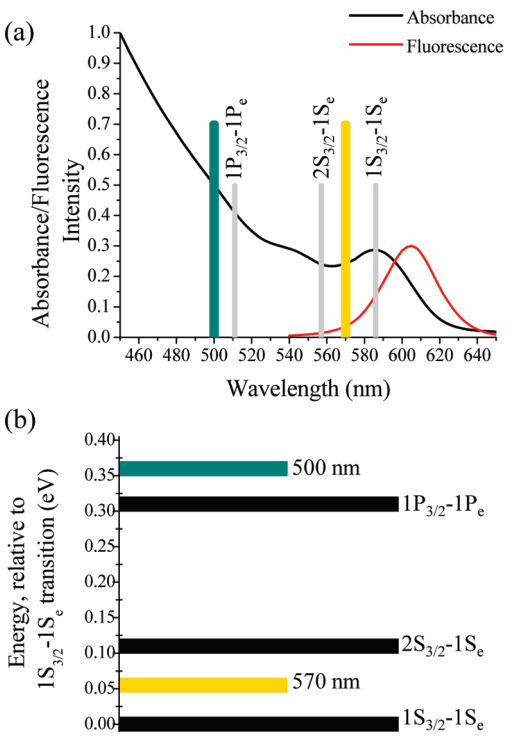

Figure 1. (a) Ensemble absorbance and fluorescence spectra of CdSe/ZnS core/shell QDs in toluene, normalized to the first absorption maximum. The excitation wavelength for the fluorescence spectrum is 500 nm. The three lowest energy transitions are indicated in gray (ref 35), and the blinking experiment excitation wavelengths are indicated by the green (500 nm) and yellow (570 nm) bars. (b) Illustration of the three lowest transition energies (black bars) and excitation energies (green and yellow bars), relative to the first transition.

The blinking statistics at high power densities, corresponding to $\langle N \rangle \geq 2$, are also compared for excitation of the lowest energy $1S_{3/2}-1S_e$ transition and the higher energy $1P_{3/2}-1P_e$ transition by tuning the excitation wavelength. The high degree of similarity in the on-duration probability distributions at the two excitation wavelengths suggests that the Auger ionization mechanism dominates the trapping process under these conditions and that the trap states accessed via Auger ionization are the same for the lowest photon energy and higher photon energy formation of the biexciton.

II. EXPERIMENTAL SECTION

The nanocrystal samples used for this study are commercial CdSe/ZnS core/shell spherical quantum dots (QD) purchased from Evident Corporation (ED-C11-tol-0600). Ensemble absorbance measurements find the lowest energy transition to occur at 586 nm (2.12 eV), see Figure 1a, corresponding to a core size of approximately 4 nm.[35] The ensemble fluorescence maximum occurs at 605 nm (2.05 eV) with a bandwidth of 36 nm, as shown in Figure 1. Excitation wavelengths 570 nm (2.18 eV) and 500 nm (2.48 eV) are selected to be just above the lowest energy $1S_{3/2}-1S_e$ transition and above the higher $1P_{3/2}-1P_e$ transition, respectively.[36] The 500 nm excitation wavelength is also chosen to lie above the excitation energy threshold previously observed in blinking studies on CdSe nanorods.[33] Figure 1b illustrates the excitation wavelength positions relative to the lower energy transitions for a CdSe quantum dot of this size, as extrapolated

from Norris and Bawendi.[35,36] The QD samples are spun or drop-cast onto UV-grade fused-silica coverslips, passivated with *N*-(2-aminoethyl)-3aminopropyltrimethoxysilane to bind the QDs, at average densities less than 0.1 QDs/μm^2, as measured from wide-field fluorescence images and atomic force microscopy (AFM).

The experimental apparatus consists of a home-built confocal fluorescence microscope used in the epifluorescence configuration. Pulsed excitation at a tunable wavelength is achieved by a Coherent Mira900 titanium sapphire oscillator producing ultrashort pulses that are amplified by a Coherent RegA9000 regenerative amplifier to produce ~200 fs pulses at 800 nm and 295 kHz repetition rate; the amplifier pumps a Coherent OPA9400 optical parametric amplifier to produce excitation pulses of tunable wavelength from 500 to 700 nm with less than 5 nm of bandwidth. For this study the average power is tunable and reduced below 10 μW by a series of interchangeable neutral density filters. The sample is mounted on piezoelectric stages to allow fine adjustments in the *xyz* axes (PI 517 two-axis and home-built single-axis stage), and the excitation light is focused onto the coverslip surface through an oil immersion objective, NA = 1.3 (Nikon PlanFluor100). Sample fluorescence is collected through the same objective and separated from any reflected excitation light by a dichroic mirror and several band-pass filters centered at 600 nm. The remaining fluorescence is directed to a single photon counting avalanche photodiode (PDM series, MPD), whose signal is input to either a multichannel scalar (SRS) or a time-correlated single photon counting (TCSPC) card (PicoHarp300, Picoquant). The fluorescence from individual dots is recorded for 20 min, after which the counts are binned into 10.5 ms bins to construct a blinking trajectory. The lifetime information available through the TCSPC card will not be referred to for this study.

The excitation intensity for each measurement is calculated from the average power measured before the objective, the repetition rate of the laser as measured by a frequency counter (Agilent 53131A), and from the spot size of the laser focus as measured daily using fluorescent dye-coated beads (Phosphorex). The average number of excitons created per excitation pulse, $\langle N \rangle$, is calculated from the excitation intensity described above and the absorption cross section, σ_λ, which is approximated as $\sigma_{500} = 1.06 \times 10^{-15}$ cm^2 or $\sigma_{570} = 8.61 \times 10^{-16}$ cm^2.[35] A wide range of power densities corresponding to $\langle N \rangle = 0.2$ to $\langle N \rangle = 6$ or more is used. It is worth noting that the repetition rate of our excitation source is considerably lower than most pulsed excitation sources used in blinking studies (which are often 1−10 MHz); this difference is key to allowing us to measure single QD fluorescence over the long, 20 min duration of the blinking experiment at high pulse intensities without photobleaching.

The data reported here represent the statistics of 140 individual quantum dots. A representative sample of the fluorescence blinking trajectories is shown in Figure 2a. The blinking trajectories are analyzed into consecutive on- and off-time durations by setting a threshold value above/below which is considered on/off. The threshold value is determined here by an off-duration region that is representative of the lowest average intensity level, such that it will certainly be considered as off. The threshold is set by adding the standard deviation of the bin intensity values to the maximum bin intensity for that off duration. This method consistently yields threshold values 3−4 standard deviations from the mean off-duration intensity. Recent work questions the validity of the bin and threshold analysis methods used here,

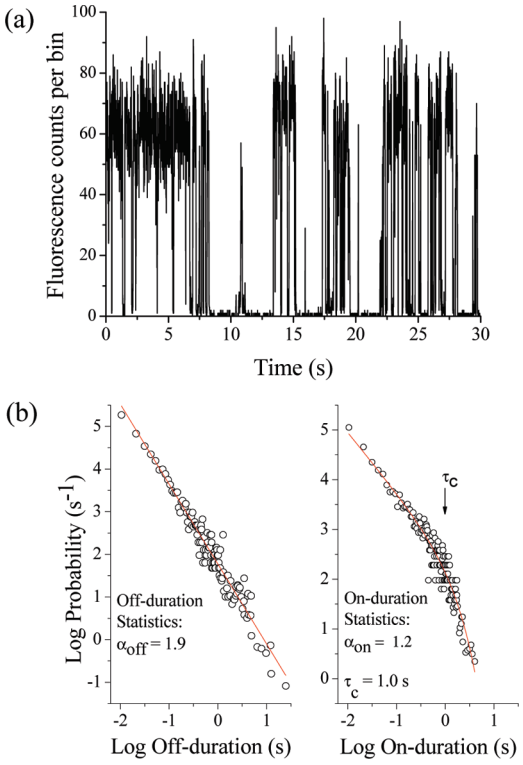

Figure 2. (a) A 30 s excerpt of a fluorescence blinking trajectory from a single CdSe/ZnS core/shell QD. The fluorescence counts are binned into 10.5 ms time bins. (b) Sample off- and on-duration probability distributions are plotted on a log−log scale. The off-duration distribution shown here adheres to a power law decay with $\alpha_{off} = 1.9$; this fit is shown in red. The on-duration probability decay is better described by eq 2 with $\alpha_{on} = 1.2$ and $\tau_c = 1.0$ s; fit also shown in red.

indicating that a change in bin size or threshold level can alter the probability distributions of the on and off durations.[37,38] While this publication was underway a more rigorous statistical analysis, change point detection (CPD), was implemented. The CPD analysis uses the individual photon arrival times to locate the statistically relevant intensity change points and number of states represented by the data; it does not require binning or thresholding.[39] A large subset of the data presented here was also analyzed using CPD. This data produces the same excitation intensity dependence in both the on- and off-duration probability distributions as is reported here.

The probability of on- and off-time durations used here is a probability density, $P(\tau_{on/off})$. The probability density weights the occurrence of the on and off event of a given duration, $N_{\tau,i}$, by the average time difference from the next longer and shorter durations.

$$P(\tau_i) = \frac{2N_{\tau,i}}{(\tau_{i+1} - \tau_i) + (\tau_i - \tau_{i-1})} \quad (1)$$

Although this method scales the common short $\tau_{on/off}$ values by the same constant, the most rare long duration events are scaled down to the smallest probability values, thus providing an estimate of the probability of these events were the experiment not of a limited duration.[40] Sample on- and off-duration probability distributions are shown in Figure 2b, plotted on a log−log scale. The probability distribution of the short on events is

well-described by an inverse power law with coefficient α_{on}, while the probability of longer on events is truncated by an exponential decay.

$$P(\tau_{on}) \propto \tau_{on}^{-\alpha_{on}} e^{\tau_{on}/\tau_c} \quad (2)$$

The crossover from power law to exponential decay is marked by the crossover time τ_c. The off-duration probabilities appear to adhere more closely to a power law distribution with a power coefficient α_{off}, but then also begin to fall off from the linear fit for longer events. These off-time data could not be well-fit to the truncated power law equation and will be discussed in more detail in the Results and Discussion section. In all cases, the $\alpha_{on/off}$ fit coefficient was found from a linear fit to the log−log plot of the data points occurring in the first 55 ms, whereas τ_c comes from a fit of the log of $P(\tau_{on})$ versus log τ_{on} derived from eq 2.

III. RESULTS AND DISCUSSION

The qualitative effect of increasing excitation intensity on the on- and off-duration probability distributions is summarized in Figure 3. The on-duration crossover time, τ_c, occurs at earlier times as the excitation intensity is increased. This same trend has been reported in several previous studies.[23−25,28−30,41] The off-duration probability distribution also diverges from the power law behavior as the excitation intensity is increased. To quantify this divergence a fit to eq 2 was attempted, but not successful, suggesting that the off-duration crossover time may occur on time scales longer than the events measured here. It is worth noting that the DCET blinking mechanism predicts the off-duration crossover to occur at substantially longer times than the on-duration τ_c.[24] Therefore, the divergence from the power law behavior is instead defined by a divergence time, τ_d, at which the log of the off-duration probability diverges by more than 0.5 s^{-1} from the power law fit calculated from the short-duration data points (first 55 ms). The value of τ_d does not provide insight into the exponential decay of the long-duration events as does the on-duration τ_c. However, both τ_c and τ_d quantify the point at which the power law description is no longer adequate, and the deviation can be compared in that regard. To verify the validity of comparing the on- and off-duration parameters, τ_c and τ_d, the divergence times for the on-time probability distributions were calculated, and all excitation intensity-dependent trends were reproduced. The observation of an off-duration crossover time from the power law behavior has been reported for CdSeTe/ZnS quantum dots under high excitation intensity conditions[29] as well as for CdSe nanorods.[31,33] It is also worth noting that an excitation intensity dependence of the off-time statistics has not been previously reported for CdSe/ZnS QDs. Power law fits to the full range of the off-time data also considered here, not taking into account the divergence of the longer-duration off

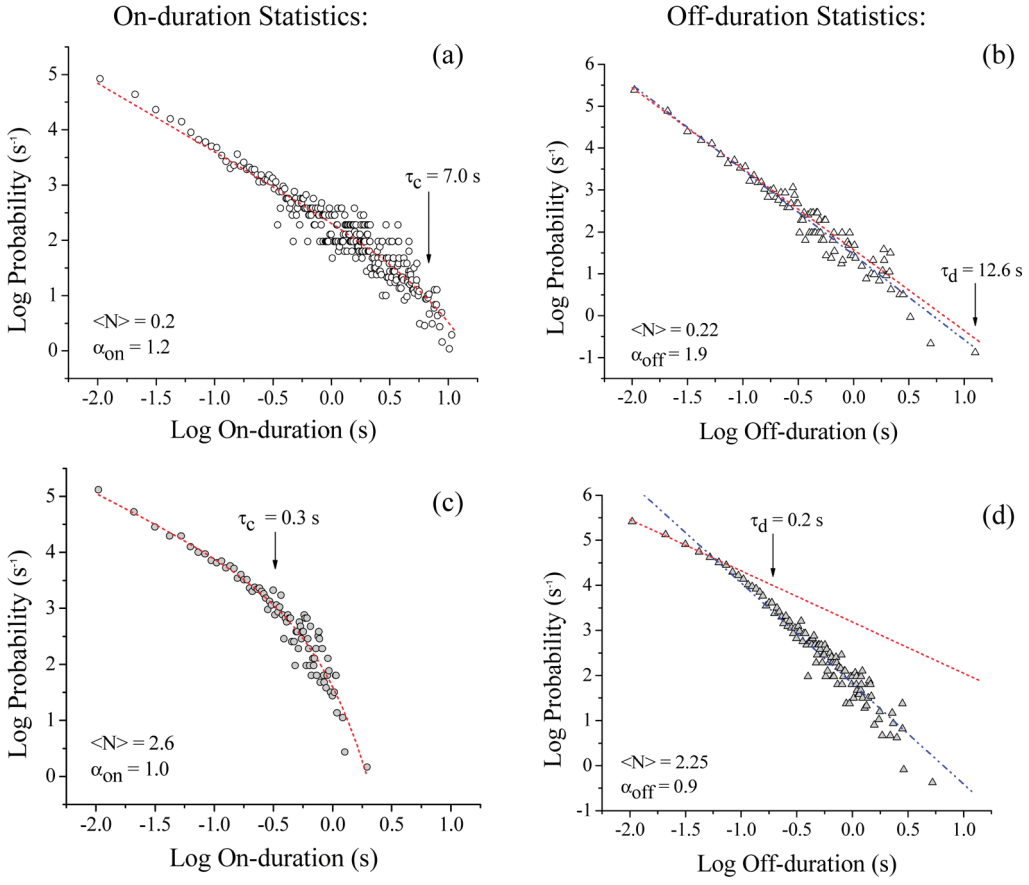

Figure 3. Sample on-duration (a and c) and off-duration (b and d) probability distributions at high and low excitation intensities corresponding to $\langle N \rangle = 0.2$ (a and b) and $\langle N \rangle > 2$ (c and d). For the on-time distributions the dashed red lines show the fits to the truncated power law in eq 2. The slope, α_{on}, is listed on the plot, and the arrows indicate τ_c (a and c). For the off-time distributions the dashed red lines show the power law fit from events shorter than 55 ms with a slope, α_{off}, listed on the plot, and the arrows indicate τ_d. The blue dot-dash lines indicate the power law fit to the entire data set, which yields $\alpha_{off} = 2.0$ (b) or $\alpha_{off} = 2.2$ (d). This fit clearly does not provide an adequate description of the high-power data.

dx.doi.org/10.1021/jp2001223 |J. Phys. Chem. C 2011, 115, 6341–6349

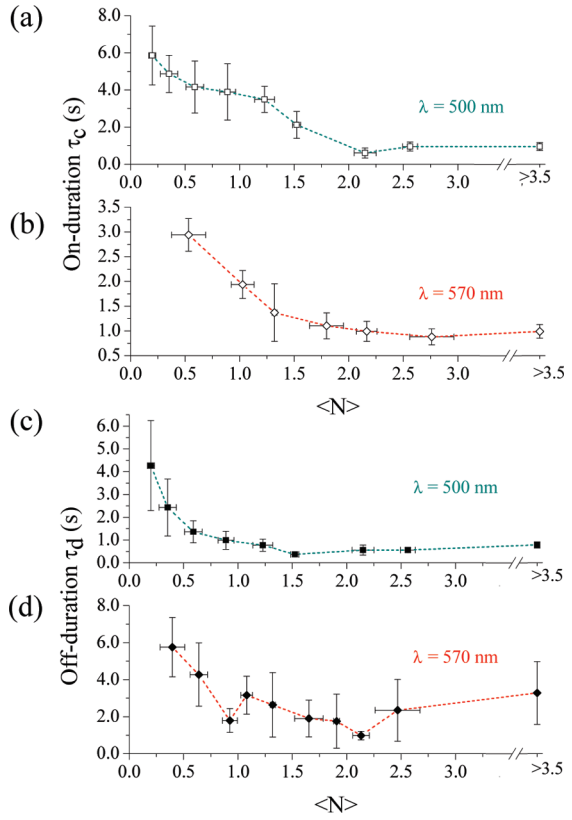

Figure 4. On-duration (a and b) and off-duration (c and d) crossover times as a function of average number of excitons per pulse with 500 nm (a and c) and 570 nm (b and d) excitation. These plots represent the fits from 62 (a and c) or 78 (b and d) trajectories taken over a range of excitation intensities, binned by $\langle N \rangle$ and averaged in the *x*- and *y*-axes. The *x*-errors are plus and minus the standard deviation of $\langle N \rangle$, and *y*-errors are plus and minus the standard deviation of the mean of τ_c or τ_d. Plots a and b show the on-duration τ_c saturates around $\langle N \rangle = 2$. Plots c and d show the off-duration τ_d saturates around $\langle N \rangle = 1$.

events, do not reveal excitation intensity dependence. However, it is clear from Figure 3d that a power law fit is not an accurate description of the data taken at higher excitation intensities.

The trends described above are quantified by the excitation intensity dependence of the fit parameters for the on- and off-duration probability distributions. Figure 4 illustrates the excitation intensity dependence of the on- and off-durations, τ_c and τ_d, respectively. Under both excitation wavelength conditions, an intensity increase leads to a decrease in the on-duration τ_c, which saturates at $\langle N \rangle \approx 2$, and a decrease in the off-duration τ_d, which saturates at $\langle N \rangle \approx 1$. We assert that there is no single blinking mechanism that can predict the different saturation points observed in the on and off blinking behavior, as discussed next. The result is evidence for two different mechanisms affecting the behavior of the QD fluorescence intermittency over the large range of excitation intensities probed here. Specifically, a trapping mechanism that involves a multiexciton species (saturation at $\langle N \rangle = 2$) and a detrapping mechanism that involves a single exciton (saturation at $\langle N \rangle = 1$) must be invoked.

First the excitation intensity dependence of the off-duration τ_d is considered. The DCET mechanism predicts the on- and off-duration crossover times to be inversely proportional to the diffusion time constant and therefore to the excitation intensity.[24,42] Spectral diffusion of the fluorescence of single QDs is also thought to stem from these energy fluctuations and has been shown to be strongly correlated to the blinking behavior,[43] possibly due to the migration of surface trapped charges.[42] The measurement of surface charging of single CdSe QDs as a function of power density by electrostatic force microscopy separately demonstrates the ionization to occur via a single-photon process at low power densities (corresponding to $\langle N \rangle \ll 0.1$).[44] A more recent mechanism that has been invoked to describe spectral diffusion and blinking is the coupling of the QD electronic levels to a two-level system (TLS) environment. In this case the TLS is multiple recombination centers at the QD surface.[37,45] In terms of blinking, this mechanism suggests that the hole accesses a distribution of multiple trapping sites that randomly switch between active and inactive states with high and low trapping rates, respectively. The hole recombines nonradiatively with the electron after each trapping event. This mechanism also predicts an intensity dependence in the on- and off-duration statistics, as it implies light-induced jumps between the two conformations of the trap sites. However, the mechanism of this switching process has not been determined.

Despite not having an accurate fit value for an off-duration crossover time, the τ_d parameter defined here qualitatively represents the same process of a divergence of long-duration off events away from the power law behavior. Considering the charging of the surface by a single-photon mechanism as the excitation intensity-dependent process for DCET leads to the conclusion that the saturation of τ_d at $\langle N \rangle \approx 1$ reasonably supports a diffusion-based component to the overall blinking mechanism. Alternatively, it is possible that this result could support the multiple recombination center model; however, it is not certain because the light-induced aspect of this mechanism has not been experimentally investigated.

Were DCET the only mechanism responsible for the excitation intensity dependence observed in the on-duration statistics, one would expect the saturation of the on-duration τ_c to also occur at $\langle N \rangle \approx 1$. The observation that τ_c saturates at $\langle N \rangle \approx 2$ (Figure 4) therefore suggests that an additional mechanism is involved in the decrease of τ_c. This is most likely a multiexciton-dependent process, as $\langle N \rangle$ saturates upon the creation of a biexciton, such as Auger ionization induced trapping. Convincing calculations introduced by Peterson and Nesbitt illustrate that, although an Auger ionization event is very unlikely on a per pulse basis at low excitation intensities, it becomes highly probable on the long time scales of the on-time durations.[28] In order to model the effect of Auger ionization induced trapping on τ_c we extend these calculations for our experimental conditions and without any assumptions of a small $\langle N \rangle$ value. We assume the decrease in the exponential decay lifetime of the on-duration probability distribution is due only to Auger ionization induced trapping and define τ_c as the lifetime (1/e time) for this process. The crossover time is therefore a function of the per pulse probability of creating a multiexciton, $P(n \geq 2)$ where n is the number of excitons, and the probability of an ionization event occurring from that multiexciton state, $P(\text{ionize})$.

$$\tau_c = \frac{\Delta T}{P(n \geq 2)P(\text{ionize})} \quad (3)$$

The laser period, ΔT, i.e., the time between laser pulses, converts these probabilities to a time scale. For the smallest power densities reported in this study, corresponding to $\langle N \rangle = 0.15$, the per pulse probability of creating a multiexciton is $P(n \geq 2) = 1.0\%$. With a

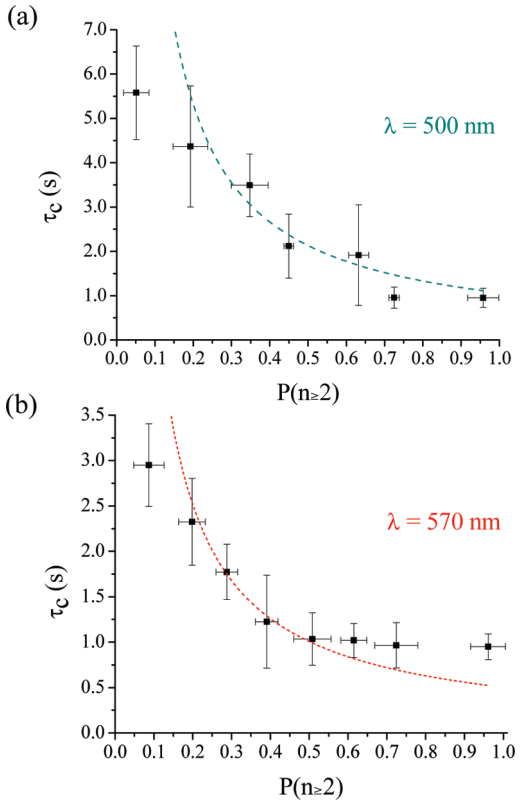

Figure 5. On-duration crossover time as a function of the per pulse probability of creating a multiexciton. These plots were made from the same data shown in Figure 2, parts a and b. The data is binned by $P(n \geq 2)$ and averaged along the *x*- and *y*-axes. The *x*-error bars are plus and minus the standard deviation of $P(n \geq 2)$. The *y*-error bars are plus and minus the standard deviation of the mean of τ_c. The dashed lines show the best fit to eq 3 with constant P(ionize) and considering only those values of $P(n \geq 2) > 0.3$. These fits yield P(ionize) values equal to $3.7 \pm 0.3 \times 10^{-6}$ for 500 nm excitation (a) and $6.3 \pm 0.3 \times 10^{-6}$ for 570 nm excitation (b).

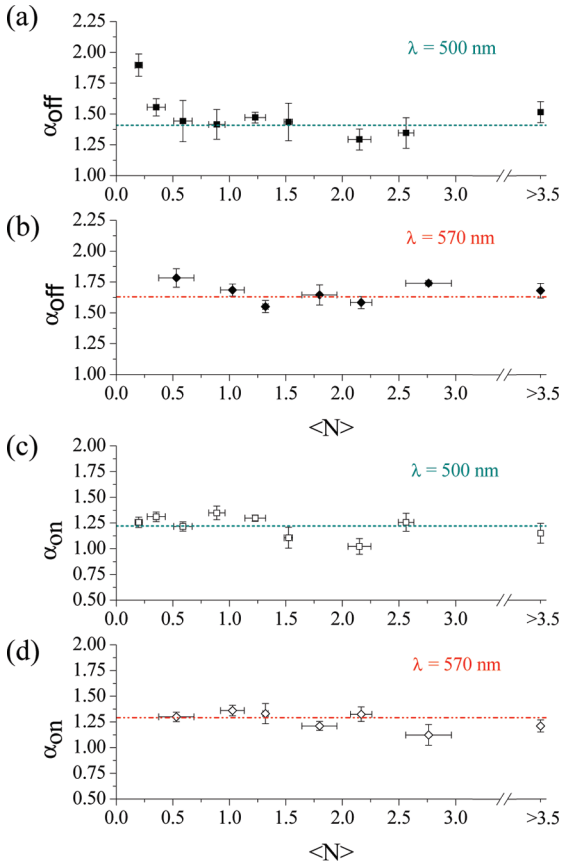

Figure 6. Off-duration (a and b) and on-duration (c and d) power law exponents as a function of average number of excitons per pulse for excitation at 500 nm (a and c) and 570 nm (b and d). These plots were made by the same analysis as Figure 2a−d. The *x*-error bars are plus and minus the standard deviation of $\langle N \rangle$, and *y*-error bars are plus and minus the standard deviation of the mean of $\alpha_{on/off}$. The dashed lines in plots a and b show the average value for all α_{off} data with $\langle N \rangle > 1$. The dashed lines in plots c and d show the average value of α_{on} over the full range of $\langle N \rangle$.

repetition rate of 295 kHz, this probability yields a multiexciton on average every 340 μs. The possibility of detrapping via an Auger ionization based mechanism is not considered here, as this would suggest that saturation of the off-duration divergence would occur at $\langle N \rangle = 2$ as well.

To fit the on-duration data to the model described above, $\langle N \rangle$ is converted to $P(n \geq 2)$ through Poisson statistics. Each absorption event is assumed to be independent. The average values of τ_c are plotted as a function of $P(n \geq 2)$, see Figure 5. It cannot be assumed that Auger ionization induced trapping is the only mechanism decreasing the on-duration τ_c. This mechanism appears to have no influence on the detrapping process, or else we would observe the saturation of the off-duration τ_d at $\langle N \rangle = 2$. Since we invoke the DCET mechanism to account for the off statistics, we acknowledge that it must have the same effect on the on-duration data, as both the process of trapping and detrapping occur from diffusion over the same coordinate. To work in a regime where the Auger mechanism is mainly responsible, we fit only the τ_c data points occurring after the DCET effect is observed to saturate in the off-time data. All data with $P(n \geq 2) > 0.26$ (corresponding to $\langle N \rangle > 1$) is fit to the model described in eq 3. In this fit P(ionize) is assumed to be a constant value, and we find it to be $3.7 \pm 0.3 \times 10^{-6}$ for the 500 nm excitation and $6.3 \pm 0.3 \times 10^{-6}$ for the 570 nm excitation. The validity of the assumption that P(ionize) is constant is tested by sorting the τ_c data by $\langle N \rangle$ and plugging these values into eq 3. This analysis is applied only to the higher power data above $\langle N \rangle = 1$ and does not yield P(ionize) values that differ by more than the standard deviation over the range of $\langle N \rangle$ values measured here. These ionization probabilities are consistent with the single-photon ionization probability of 5×10^{-6}, as measured by electrostatic force microscopy.[44] An ionization probability ~10 times larger than the one reported here was calculated by Peterson and Nesbitt from blinking results conducted at much lower power densities.[28] Including the full range of the data presented here yields $P(\text{ionize}) = 1 \times 10^{-5}$. Although this P(ionize) is closer in value to the probability reported by Peterson and Nesbitt it does not account for any additional mechanisms that decrease τ_c in the single-exciton range ($\langle N \rangle < 1$).

Diffusion-based mechanisms, including DCET, can also account for the excitation intensity dependence of the on-duration τ_c at low excitation intensities. In this single-exciton regime it is not possible to separate the intensity dependence of the DCET mechanism from that of the Auger ionization mechanism; however, this is the first time that fluorescence blinking from

Table 1. Fit Results of the Average On- and Off-Duration Statistics with High Excitation Intensity Conditions[a]

	on-duration		off-duration	
excited transition (wavelength)	α_{on}	τ_c (s)	α_{off}	τ_d (s)
$1S_{3/2}-1S_e$ (570 nm)	1.2 ± 0.1	1.2 ± 0.2	1.7 ± 0.1	2.5 ± 0.7
$1P_{3/2}-1P_e$ (500 nm)	1.2 ± 0.1	1.1 ± 0.2	1.6 ± 0.1	0.8 ± 0.1

[a] High excitation intensity data is in the multiexciton regime, as shown in Figure 7. The averaged data is analyzed by averaging the probability distributions of all data with $\langle N \rangle \geq 2.5$. The data collected with 500 nm excitation represents the averaging of the probability distributions from 13 individual QDs. The data collected with 570 nm excitation represents the averaging of the probability distributions of 20 individual QDs. The errors reported here are plus and minus the standard deviation of the mean.

single QDs has been measured at such high excitation intensities. The saturation of the on-duration τ_c at $\langle N \rangle \approx 2$ provides direct evidence of charge trapping due to a multiphoton process, such as Auger ionization induced trapping.

An additional trend that is excitation intensity-dependent is observed via a decrease of the off-duration power law exponent, α_{off}, with increasing excitation intensity in the 500 nm data set, see Figure 6a. This trend is not observed in the 570 nm data, but we cannot exclude the possibility that it also exists in Figure 6b, since the lowest $\langle N \rangle$ measured for 570 nm is above the saturation value for the 500 nm data. The on-duration power law exponent, α_{on}, shows no excitation intensity dependence at either wavelength, see Figure 6, parts c and d. Neither DCET nor Auger ionization induced trapping predict any excitation intensity dependence for the power law portion of the blinking behavior. This leads us to conclude that there may be a difference in the mechanisms that lead to the short on- and off-duration events that determine the values of α. Similar intensity-dependent trends have been reported in the blinking statistics of CdSeTe/ZnS QDs embedded in a polymer host.[29] However, this effect was attributed to a transient change in the dielectric constant of the polymer film in which the QDs were embedded. As the QDs used here are not embedded in a polymer film, this model is not considered. Also the excitation intensity dependence in the on-duration α_{on} is not observed, contrary to those previous measurements. A power law exponent larger than 3/2 has been predicted by introducing anomalous diffusion with a time-dependent diffusion constant into the DCET model.[24,46] The data suggests that anomalous diffusion may be necessary to describe the off-duration blinking statistics at low powers, but not the on-duration statistics. It is also possible that the decrease in the slope of the short off-duration events at higher intensities is simply a shift from the more distributed power law kinetics to an exponential distribution, which would have a smaller slope at durations less than the crossover time.

Finally, the blinking behavior observed in the multiexciton regime is compared for the two excitation wavelengths used: 570 and 500 nm. These wavelengths correspond to excitation of the $1S_{3/2}-1S_e$ and the $1P_{3/2}-1P_e$ transitions, respectively. Previous transient absorption experiments at several excitation wavelengths on CdSe QD ensembles in solution report enhanced trapping from the excited biexciton state ($\langle N \rangle \geq 2$). They conclude that direct trapping from the excited biexciton state competes with relaxation to the band edge.[47] This result suggests that one might observe differences in the blinking statistics when

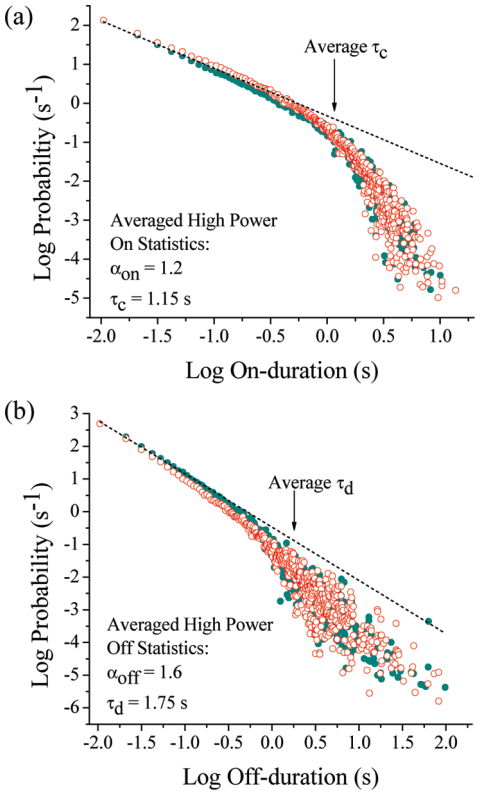

Figure 7. Aggregated on-duration (a) and off-duration (b) probability distributions measured with high excitation intensities in the multiexciton regime. The data with excitation at 500 nm is shown in green (filled-in circles). The data with 570 nm excitation is shown in red (open circles). The dashed lines illustrate the power law decays calculated from the short on/off events (less than 55 ms) with a power law exponent indicated by $\alpha_{on/off}$ and arrows indicating the crossover time or divergence time, τ_c and τ_d.

generating excited-state versus ground-state biexcitons. Comparison of the on- and off-duration probability distributions upon excitation of the $1S_{3/2}-1S_e$ (570 nm) and the $1P-1P_e$ (500 nm) transitions with $\langle N \rangle \geq 2.5$ yields little difference, see fit results in Table 1. Although some 500 and 570 nm fit parameters are not within the error bars, the overlaid average probability distributions at each wavelength highlight the degree of similarity, Figure 7. This suggests that there is no difference in the trapping and detrapping mechanisms of an excited- or ground-state biexciton.

This result contrasts several previous low-power studies comparing the blinking statistics of rod and spherical nanocrystals at several excitation wavelengths. Those studies indicated enhanced trapping when the excitation energy was in excess of the band gap.[33,34,41] In the case of uncapped CdSe nanorod blinking, Knappenberger et al. found that excitation 240 meV above the band gap led to a decrease in the on-duration τ_c by a factor of ~4.5. They concluded that the excess excitation energy permits access to external trapping sites.[33] The excitation power densities used in the studies cited above all correspond to $\langle N \rangle \leq 0.15$ per pulse or per fluorescence lifetime. The data compared here corresponds to core/shell QDs excited in the multiexciton regime with $\langle N \rangle > 2.5$; therefore, the wavelength-independent outcome at the high excitation intensities here does not contradict those cited above. The wavelength-independent results reported here instead suggest that the mechanism that governs

dx.doi.org/10.1021/jp2001223 |J. Phys. Chem. C 2011, 115, 6341–6349

blinking in this multiexciton regime is not affected by excitation wavelength. It is possible that the Auger ionization process provides enough energy to access these external sites, which at lower excitation intensities could only be accessed with a more energetic photon. If this is the case, then the passivation of the CdSe QDs with a ZnS shell did not prevent surface sites from being accessed.

A qualitative comparison of the excitation intensity dependence of the blinking parameters over the range of $\langle N \rangle$ values used in this study does not indicate any major differences between the two wavelength excitation conditions. Saturation of the on-duration τ_c occurs at $\langle N \rangle \approx 2$, whereas saturation of the off-duration τ_d occurs at $\langle N \rangle \approx 1$ for both wavelengths, Figure 4. However, it is worth noting a small difference in on-duration τ_c versus $P(n \geq 2)$ trend, shown in Figure 5, in that τ_c appears to saturate beyond $P(n \geq 2) \approx 0.5$ rather than continuing to decrease as eq 3 predicts. For the 500 nm excitation, τ_c is modeled as a function of the probability of creating any higher order exciton state, $P(n \geq 2)$. The difference in the 570 nm excitation is likely because the $1S_{3/2}-1S_e$ transition is excited and the $1S_e$ state is only doubly degenerate with respect to its spin projection;[36] therefore, it is not possible to create any multiexciton states higher than $n = 2$. The effect of this limitation could be the saturation observed in τ_c as a function of $P(n \geq 2)$.

IV. CONCLUSIONS

In conclusion, the excitation intensity dependence of the blinking behavior of single CdSe/ZnS QDs is monitored over a wide range of power densities (corresponding to $\langle N \rangle$ from 0.2 to >3) using two excitation wavelengths (500 and 570 nm). Both the on- and off-duration probability distributions diverge from power law behavior for long on/off-duration events. The off-duration divergence is shown to saturate at $\langle N \rangle = 1$, whereas the on-duration divergence saturates at $\langle N \rangle = 2$. The difference in saturation points of the on- and off-probabilities requires multiple trapping and detrapping mechanisms to be invoked. The off-duration saturation upon creation of single exciton ($\langle N \rangle = 1$) can be explained by diffusion-based blinking mechanisms that rely on surface charging, as this has been shown to occur by a single-photon process,[44] for example, DCET. A second mechanism must be invoked to explain the delayed saturation point for the on-duration statistics at $\langle N \rangle = 2$. The saturation upon creation of a biexciton suggests a multiexciton-induced trapping process. The on-duration crossover time, τ_c, is modeled in the framework of Auger ionization induced trapping and fit to the experimental data in the range of $\langle N \rangle > 1$. The wide range of power densities used here and the saturation of τ_c upon the creation of a biexciton is evidence of a multiexciton-induced trapping process, such as Auger ionization.

The blinking statistics in the multiexciton regime are also compared as a function of excitation wavelength. No difference is observed in the on- and off-probability distributions upon excitation of the $1S_{3/2}-1S_e$ or $1P_{3/2}-1P_e$ transition. This result suggests that the sites accessed via Auger ionization induced trapping are the same regardless of creating an initially excited- or ground-state biexciton.

AUTHOR INFORMATION

Corresponding Author

*Phone: 510-643-5467. Fax: 510-643-1376. E-mail: srl@berkeley.edu.

ACKNOWLEDGMENT

The authors gratefully acknowledge financial support by the Director, Office of Science, Office of Basic Energy Sciences, U.S. Department of Energy under contract no. DE-AC02-05CH11231 through the Division of Materials Research. Partial financial support for T.J.B. was provided by the Laboratory Directed Research and Development program at Lawrence Berkeley National Laboratory.

REFERENCES

(1) Colvin, V. L.; Schlamp, M. C.; Alivisatos, A. P. *Nature* **1994**, *370*, 354–357.
(2) Sun, Q.; Wang, Y. A.; Li, L. S.; Wang, D.; Zhu, T.; Xu, J.; Yang, C.; Li, Y. *Nat. Photonics* **2007**, *1*, 717–722.
(3) Coe, S.; Woo, W.-K.; Bawendi, M.; Bulovic, V. *Nature* **2002**, *420*, 800–803.
(4) Klimov, V. I.; Mikhailovsky, A. A.; Xu, S.; Malko, A.; Hollingsworth, J. A.; Leatherdale, C. A.; Eisler, H.-J.; Bawendi, M. G. *Science* **2000**, *290*, 314–317.
(5) Huang, M. H.; Mao, S.; Feick, H.; Yan, H.; Wu, Y.; Kind, H.; Weber, E.; Russo, R.; Yang, P. *Science* **2001**, *292*, 1897–1899.
(6) Bruchez, M., Jr.; Moronne, M.; Gin, P.; Weiss, S.; Alivisatos, A. P. *Science* **1998**, *281*, 2013–2016.
(7) Talapin, D. V.; Lee, J.-S.; Kovalenko, M. V.; Shevchenko, E. V. *Chem. Rev.* **2010**, *110*, 389–458.
(8) Huynh, W. U.; Dittmer, J. J.; Alivisatos, A. P. *Science* **2002**, *295*, 2425–2427.
(9) Law, M.; Greene, L. E.; Johnson, J. C.; Saykally, R.; Yang, P. *Nat. Mater.* **2005**, *4*, 455–459.
(10) Gur, I.; Fromer, N. A.; Geier, M. L.; Alivisatos, A. P. *Science* **2005**, *310*, 462–465.
(11) Zhao, J.; Nair, G.; Fisher, B. R.; Bawendi, M. G. *Phys. Rev. Lett.* **2010**, *104*, 157403.
(12) Rosen, S.; Schwartz, O.; Oron, D. *Phys. Rev. Lett.* **2010**, *104*, 157404.
(13) Kuno, M.; Fromm, D. P.; Johnson, S. T.; Gallagher, A.; Nesbitt, D. J. *Phys. Rev. B* **2003**, *67*, 125304.
(14) Cichos, F.; Borczyskowski, C. v.; Orrit, M. *Curr. Opin. Colloid Interface Sci.* **2007**, *12*, 272–284.
(15) Frantsuzov, P.; Kuno, M.; Janko, B.; Marcus, R. A. *Nat. Phys.* **2008**, *4*, 519–522.
(16) Efros, A. L. *Nat. Mater.* **2008**, *7*, 612–613.
(17) Lee, S. F.; Osborne, M. A. *ChemPhysChem* **2009**, *10*, 2174–2191.
(18) Stefani, F. D.; Hoogenboom, J. P.; Barkai, E. *Phys. Today* **2009**, *62*, 34–39.
(19) Krauss, T. D.; Peterson, J. J. *J. Phys. Chem. Lett.* **2010**, *1*, 1377–1382.
(20) Nirmal, M.; Dabbousi, B. O.; Bawendi, M. G.; Macklin, J. J.; Trautman, J. K.; Harris, T. D.; Brus, L. E. *Nature* **1996**, *383*, 802–804.
(21) Efros, A. L.; Rosen, M. *Phys. Rev. Lett.* **1997**, *78*, 1110–1113.
(22) Kuno, M.; Fromm, D. P.; Hamann, H. F.; Gallagher, A.; Nesbitt, D. J. *J. Chem. Phys.* **2000**, *112*, 3117–3120.
(23) Shimizu, K. T.; Neuhauser, R. G.; Leatherdale, C. A.; Empedocles, S. A.; Woo, W. K.; Bawendi, M. G. *Phys. Rev. B* **2001**, *63*, 205316.
(24) Tang, J.; Marcus, R. A. *J. Chem. Phys.* **2005**, *123*, 054704.
(25) Lee, D.-H.; Yuan, C.-T.; Tachiya, M.; Tang, J. *Appl. Phys. Lett.* **2009**, *95*, 163101.
(26) Lee, J. D.; Maenosono, S. *J. Chem. Phys.* **2010**, *133*, 074703.
(27) Banin, U.; Bruchez, M.; Alivisatos, A. P.; Ha, T.; Weiss, S.; Chemla, D. S. *J. Chem. Phys.* **1999**, *110*, 1195–1201.
(28) Peterson, J. J.; Nesbitt, D. J. *Nano Lett.* **2009**, *9*, 338–345.
(29) Goushi, K.; Yamada, T.; Otomo, A. *J. Phys. Chem. C* **2009**, *113*, 20161–20168.
(30) Stefani, F. D.; Knoll, W.; Kreiter, M.; Zhong, X.; Han, M. Y. *Phys. Rev. B* **2005**, *72*, 125304.

(31) Tang, J. *J. Phys. Chem. A* **2007**, *111*, 9336–9339.
(32) Wang, S.; Querner, C.; Emmons, T.; Drndic, M.; Crouch, C. H. *J. Phys. Chem. B* **2006**, *110*, 23221–23227.
(33) Knappenberger, K. L., Jr.; Wong, D. B.; Xu, W.; Schwartzberg, A. M.; Wolcott, A.; Zhang, J. Z.; Leone, S. R. *ACS Nano* **2008**, *2*, 2143–2153.
(34) Knappenberger, K. L., Jr.; Wong, D. B.; Romanyuk, Y. E.; Leone, S. R. *Nano Lett.* **2007**, *7*, 3869–3874.
(35) Yu, W. W.; Qu, L.; Guo, W.; Peng, X. *Chem. Mater.* **2003**, *15*, 2854–2860.
(36) Norris, D. J.; Bawendi, M. G. *Phys. Rev. B* **1996**, *53*, 16338–16346.
(37) Frantsuzov, P. A.; Volkan-Kacso, S.; Janko, B. *Phys. Rev. Lett.* **2009**, *103*, 207402.
(38) Crouch, C. H.; Sauter, O.; Wu, X.; Purcell, R.; Querner, C.; Drndic, M.; Pelton, M. *Nano Lett.* **2010**, *10*, 1692–1698.
(39) Watkins, L. P.; Yang, H. *J. Phys. Chem. B* **2005**, *109*, 617–628.
(40) Kuno, M.; Fromm, D. P.; Hamann, H. F.; Gallagher, A.; Nesbitt, D. J. *J. Chem. Phys.* **2001**, *115*, 1028–1040.
(41) Crouch, C. H.; Mohr, R.; Emmons, T.; Wang, S.; Drndic, M. *J. Phys. Chem. C* **2009**, *113*, 12059–12066.
(42) Empedocles, S. A.; Bawendi, M. G. *J. Phys. Chem. B* **1999**, *103*, 1826–1830.
(43) Neuhauser, R. G.; Shimizu, K. T.; Woo, W. K.; Empedocles, S. A.; Bawendi, M. G. *Phys. Rev. Lett.* **2000**, *85*, 3301–3304.
(44) Krauss, T. D.; O'Brien, S.; Brus, L. E. *J. Phys. Chem. B* **2001**, *105*, 1725–1733.
(45) Plakhotnik, T.; Fernee, M. J.; Littleton, B.; Rubinsztein-Dunlop, H.; Potzner, C.; Mulvaney, P. *Phys. Rev. Lett.* **2010**, *105*, 167402.
(46) Tang, J.; Marcus, R. A. *Phys. Rev. Lett.* **2005**, *95*, 107401.
(47) Sewall, S. L.; Cooney, R. R.; Anderson, K. E. H.; Dias, E. A.; Sagar, D. M.; Kambhampati, P. *J. Chem. Phys.* **2008**, *129*, 084701.